Physics and Imaging in Radiation Oncology 17 (2021) 77–83

Contents lists available at ScienceDirect

Physics and Imaging in Radiation Oncology

journal homepage: www.sciencedirect.com/journal/physics-and-imaging-in-radiation-oncology

Original Research Article

Exploratory models comparing ethiodized oil-glue and gold fiducials for bladder radiotherapy image-guidance

Daryl Lim Joon [a,b], Alexandra Berlangieri [a], Benjamin Harris [a], Mark Tacey [a], Rachel O'Meara [a], Brent Pitt [a], Angela Viotto [a], Kerryn Brown [a], Michal Schneider [b], Nathan Lawrentschuk [a], Shomik Sengupta [a], Colleen Berry [a], Trish Jenkins [a], Michael Chao [a], Morikatsu Wada [a], Farshad Foroudi [a], Vincent Khoo [a,b,c,*]

[a] Olivia Newton John Cancer Center, Radiation Oncology, 145 Studley Rd, Heidelberg, Victoria 3084, Australia
[b] Monash University, Department of Medical Imaging and Radiation Sciences, Faculty of Medicine, Nursing and Health Sciences, Wellington Rd, Clayton, Victoria 3800, Australia
[c] Royal Marsden NHS Foundation Trust, 203 Fulham Rd, Chelsea, London SW3 6JJ, United Kingdom

ARTICLE INFO

Keywords:
Bladder cancer
Prostate cancer
Radiotherapy
Glue fiducials
Liquid fiducials
Image-guided radiotherapy

ABSTRACT

Background and purpose: Image-guidance with fiducials has been shown to improve pelvic radiotherapy outcome. However, bladder fiducials using ethiodized oil (EO) alone can disperse widely, and gold causes Computed Tomography scan (CT) metal artifacts. The study's purpose was to investigate the ability to deliver EO-tissue glue fiducials and compare them to gold for bladder radiotherapy image guidance.
Materials and methods: A fluid-filled porcine bladder model was used to assess the ability to cystoscopically inject visible EO glue fiducials into the submucosa. We then transferred the bladders into a porcine pelvis for imaging and compared them to gold fiducials using CT, Cone Beam CT (CBCT), and kilovoltage (KV) planar views. A tissue-equivalent phantom was utilized to analyze the CT number Hounsfield Unit (HU) characteristics and artifacts of the glue and gold fiducials. Percentile ranges and normal tissue voxel percentages of the subsequent CT number voxel histogram from a 2 cm sphere surrounding the fiducial was used to characterize the artifact.
Results: We successfully delivered all EO glue fiducials into the porcine bladders as discrete fiducials. They were well seen on CT, CBCT, and KV imaging. The glue fiducials had lower CT number values, but less CT number spread of the voxel percentile ranges consistent with the diminished contrast and less artifact than gold. The glue fiducial types had similar CT number characteristics.
Conclusion: This study has shown that EO glue fiducials can be delivered with online visualization qualities comparable to gold fiducials without metal-related artifacts.

1. Introduction

The bladder is a mobile structure that can expand and contract depending on its relative filling volume. Subsequently, there has been an increasing interest in using fiducials for bladder image-guided radiotherapy. Gold fiducials are the benchmark for visibility with X-ray imaging and have been used for both bladder tumors and prostate bed radiotherapy [1]. However, they produce a substantial artifact as a result of multiple mechanisms, including beam hardening, scatter, Poisson noise, motion, and edge effects [2,3]. The artifact can interfere with the accurate fiducial definition leading to imprecise image guidance. Alternatively, ethiodized oil (EO) has been utilized as a liquid fiducial for bladder tumors, but it can be challenging to achieve a discrete marker due to dispersion [4,5].

Gastroenterologists routinely use a mixture of EO and cyanoacrylate tissue glue to treat gastric and oesophageal varices [6,7]. EO is an X-ray

* Corresponding author at: Royal Marsden NHS Foundation Trust, 203 Fulham Rd, Chelsea, London SW3 6JJ, United Kingdom.
E-mail addresses: daryl.limjoon@austin.org.au (D. Lim Joon), alexandra.berlangieri@austin.org.au (A. Berlangieri), benjamin.harris@austin.org.au (B. Harris), mark.tacey@austin.org.au (M. Tacey), rachel.omeara@austin.org.au (R. O'Meara), brent.pitt@austin.org.au (B. Pitt), angela.viotto@austin.org.au (A. Viotto), kerryn.brown@austin.org.au (K. Brown), michal.schneider@monash.edu (M. Schneider), colleen.berry@austin.org.au (C. Berry), trish.jenkins@austin.org.au (T. Jenkins), michael.chao@austin.org.au (M. Chao), morikatsu.wada@austin.org.au (M. Wada), Farshad.Foroudi@austin.org.au (F. Foroudi), vincent.khoo@rmh.nhs.uk (V. Khoo).

https://doi.org/10.1016/j.phro.2021.01.008
Received 22 July 2020; Received in revised form 23 January 2021; Accepted 28 January 2021
Available online 6 February 2021

oily contrast agent that prevents the glue from initially polymerizing [6,8]. The glue rapidly sets once injected into the body and contacts water, e.g., blood, [6]. We previously have illustrated its utility as a fiducial for oesophageal cancer patients [9]. The tissue glue reduced EO's dispersion through the esophagus' wall, increasing the ability to produce a discrete visible fiducial.

While the gastroscopic insertion of EO and cyanoacrylate glue for the esophagus is well described, there are no reports of the cystoscopic delivery of tissue glues into a fluid-filled bladder. The cystoscopic insertion of a tissue glue into a watery environment raised concerns that the glue could polymerize prematurely. The glue could obstruct the needle tip, making it difficult to inject into the bladder submucosa. The premature polymerization may also glue the cystoscope's lens or channels, permanently damaging an expensive instrument, as has been reported with oesophageal varices [10].

The aim of this study was to investigate the ability to deliver visible discrete EO-tissue glue fiducials suitable for image guidance and characterize and compare them in terms of visibility and artifact production to the standard gold fiducials for bladder radiotherapy image guidance.

2. Material and methods

2.1. Glue fiducials

The glue fiducials consisted of a mixture of EO (Lipiodol Ultra liquid, esterized poppy seed oil, Aspen Medical) with either Histoacryl (monomeric n-butyl-2-cyanoacrylate, B Braun) (CA) or Glubran2 (n-butyl cyanoacrylate and methacryloxysulpholen monomers, GEM) (CM), in a 1:1 ratio, respectively.

2.2. Porcine model: image guidance visibility

The fiducial insertion utilized a 17fr rigid cystoscope that was initially used to inspect and then fill three ex-vivo porcine bladders with saline. Then a three sets of three EO/CA (EC) fiducials, three EO/CM (EM) fiducials and three gold fiducials were cystoscopically inserted into the three separate porcine bladders. A William's needle (Cook Medical, Australia) was inserted via the scope and used to inject EO glue combinations submucosally, raising a bleb of 0.1 ml. Each set of three discrete fiducials was placed around each bladder's trigone, imitating the demarcation of a small bladder tumor or the vesicourethral anastomosis following a prostatectomy. Further details of the procedure have been previously described [11].

Following the injection, the cystoscope was removed from the bladder, keeping the needle beyond the scope to avoid the glue occluding the working channel. The glue fiducials were compared with three standard gold fiducials (0.9 mm × 3 mm, CIVCO Medical Solutions, Kalona, Iowa, USA) in terms of their visibility.

Following the fiducials' insertion, the porcine bladders were transferred sequentially into a porcine pelvis (Fig. 1). The porcine pelvis was to provide realistic size and tissue densities, including inhomogeneities for imaging. According to clinical protocols, the pelvis was stabilized

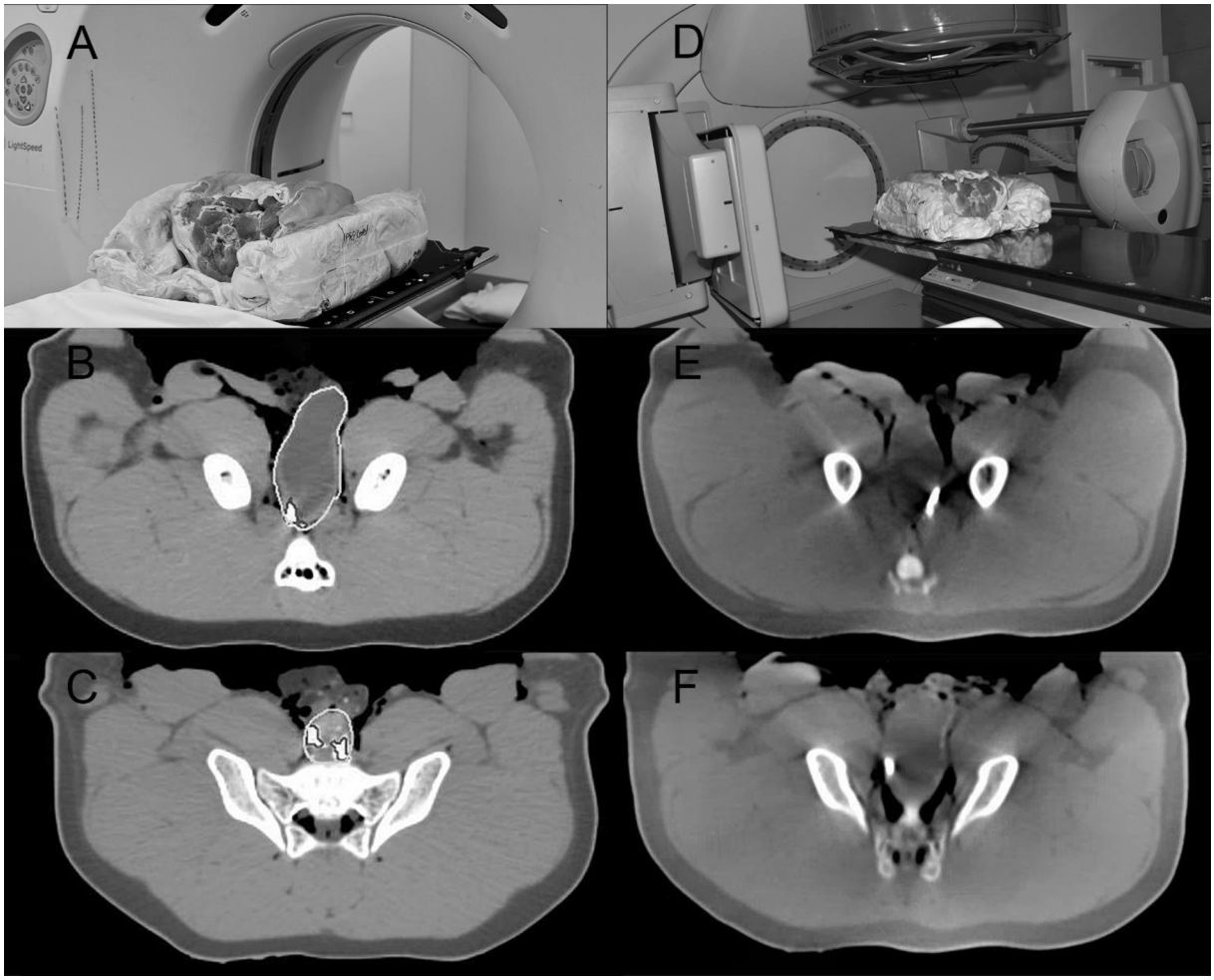

Fig. 1. Porcine Model: Pigs bladder & pelvis in two-part foam immobilization. A) CT simulation. Axial CT image with contoured bladder and fiducial showing visible B) EC fiducial and C) EM fiducial. D) Linac for cone-beam CT (CBCT) scan. Axial CBCT image showing a visible E) EC fiducial and F) EM fiducial. Abbreviations: EC: ethiodized oil and monomeric n-butyl-2-cyanoacrylate, EM: ethiodized oil and n-butyl cyanoacrylate and methacryloxysulpholen monomers.

and set up in a two-part foam immobilization device for reproducibility.

The porcine pelvis with the bladder was then imaged using radiotherapy imaging modalities, including computed tomography (CT), cone-beam computed tomography (CBCT) (Fig. 1), and kilovoltage (KV) planar imaging using standard clinical parameters for pelvic radiotherapy.

The CT simulation was performed on a GE Lightspeed RT CT (Boston, Massachusetts, USA) 1.25 mm slice width, helical, 0.75 pitch, no gap, 512x512 axial resolution, 650 mm reconstruction diameter.

CBCT was imaged on an Elekta Infinity linear accelerator (Stockholm, Sweden). The standard abdomen/pelvis scans parameters were used, i.e., 41 cm diameter FOV, variable M10/M20 (scan length 12 or 24 cm) depending on target size, 120 kVp, 25 mA 40 ms nominal per frame, 660 frames per scan (360 degrees rotation), 1 mm voxel size, 2–3 mm viewing slice resolution and axial resolution of 512 × 512.

2D orthogonal KV planar imaging was performed using anterior-posterior (AP) and lateral views. The Elekta XVI (version 4.5+) KV imaging parameters were 120 kVp, 25 (AP) or 32 (lateral) mA, and 40 ms nominal per frame, and five frames averaged per image, 25.6 × 25.6 cm imaging area, 0.25 mm nominal pixel size (Resolution 1024 × 1024).

Two expert radiation therapists who routinely verify pelvic radiotherapy independently scored the fiducials while blinded to the mixture's identity and each other to measure the fiducial visibility and minimize observer error and bias. The ability to deliver a suitable fiducial set for radiotherapy image verification was scored 0, not sufficiently visible for verification, or 1, sufficiently visible for verification for each imaging modality, CT, CBCT, and KV planar scans.

2.3. Phantom model: fiducial and artefact characterization

A CIRS Torso (tissue equivalent) phantom was used to characterize the glue fiducials and artifacts. A gold fiducial was used as the standard and embedded centrally in a wax block cylinder measuring 6.3 × 1.0 cm for comparison. A wax block cylinder alone was used as a normal tissue control. These wax blocks were constructed and inserted to minimize any air gaps with the phantom.

Further tissue-equivalent, wax block cylinders were constructed for the glue fiducials. Holes for the glue fiducials were drilled into individual blocks that approximated (1) the size of the 0.1 ml porcine bladder glue fiducials, i.e., large, 7 × 4 mm, and (2) the size of the gold fiducials, i.e., small, 0.9 × 3 mm. The holes were moistened for polymerization and then filled with the glue fiducial. A small EO alone fiducial control was also created. Each wax cylinder was then sequentially inserted into the CIRS phantom center and imaged on CT using the same clinical parameters as the porcine model. Two fiducial samples were used for each control, gold, and large glue fiducials. Four samples were created for the small glue fiducials, to account for any possible variation due to their small size (Table 1).

2.4. Fiducial and artefact analysis & statistical description

CT number Hounsfield number (HU) histograms are increasingly used to analyze human tissue characteristics [12–14]. Subsequently, a methodology using CT number histograms derived from clinical tools, i.e., MIM Maestro version 6.6.13 (Cleveland OH, USA) (MIM), was developed to analyze the fiducial artifacts in a three-dimensional manner consistent with modern radiotherapy.

The fiducials were contoured as per clinical protocols using a window level that approximated fiducial size, i.e., window level of 4095 with a width one and gamma [15,16] of one for the gold fiducials and level of 600 with a width of 40 and gamma of one for the polymer. Then a 2 cm diameter sphere was created around the fiducial contour center. The high CT number fiducials were subtracted from the sphere using a Boolean function to analyze the artifact's impact on normal tissue. The CT number voxel histogram for the artifact sphere was then exported in 5 HU bins for analysis. The fiducials' CT number characteristics were separately investigated as they produced very high CT number signals compared to the artifact.

The spheres contained the phantom, surrounding wax, and the relevant fiducial seed's 3D artifact. MIM was used to create histogram plots, presenting the voxels count at each CT number (HU) value to assess the relative differences in CT number variation surrounding each fiducial marker.

Given the non-normal, bi-modal distribution of the voxel count histograms, means and standard deviations were not suitable for describing and comparing the histograms across the fiducial marker type. Therefore, the variation in voxel counts in the spheres (excluding the fiducial) were measured with percentile ranges. An example of the percentiles range is illustrated in Fig. 2 using the wax control fiducial. Additionally, the normal tissue not hidden by artifact was quantified by the proportion of voxels within the normal tissue CT number ranges of +/−100 HU and +/−150 HU.

No statistical significance was assigned due to the small sample size for this descriptive study. Data was collected and prepared in Microsoft Excel. Stata version 15.1 (College Station, Texas, USA) was used to calculate CT number parameters, percentile ranges, and proportions.

3. Results

3.1. Porcine bladder model: fiducial deliverability & visibility

The gold fiducials were well visualized on all imaging modalities. EO glue combinations could be injected repeatedly into the porcine bladder submucosa, raising consistent multiple small blebs. They were larger than the gold fiducials measuring approximately 7 × 4 mm, being overall elliptical in shape. All three fiducials for both EC and EM fiducials could be visualized on CT, CBCT, and KV imaging that was adequate for verification. The EC and EM fiducials' appearances were similar on CT and CBCT (Fig. 1).

Table 1
Phantom Model: Comparison of the Fiducial and Controls in terms of volume, voxel number, and CT number Hounsfield Unit (HU) characteristics. It illustrates that the gold fiducials had a greater CT number HU contrast than the small glue fiducials with a comparable volume and voxel number. Abbreviations: EO: ethiodized oil, EC: ethiodized oil and monomeric n-butyl-2-cyanoacrylate, EM: ethiodized oil and n-butyl cyanoacrylate and methacryloxysulpholen monomers.

Fiducial/Factor	Number Of Fiducials	Volume cm^3 (average)	Voxel number (average)	Median CT number (HU)	Min CT number (HU)	Max CT number (HU)
Control (2 cm phantom sphere alone)	2	3.85	1912	24	−220	79
Control (Wax)	2	0.02	9	−24	−114	57
EO alone	2	0.02	9	346	0	1383
Gold	2	0.02	8	6039	1229	16,779
Small EC	4	0.02	6	374	50	642
Small EM	4	0.02	6	488	25	835
Large EC	2	0.08	38	717	−261	2092
Large EM	2	0.07	35	770	−22	2472

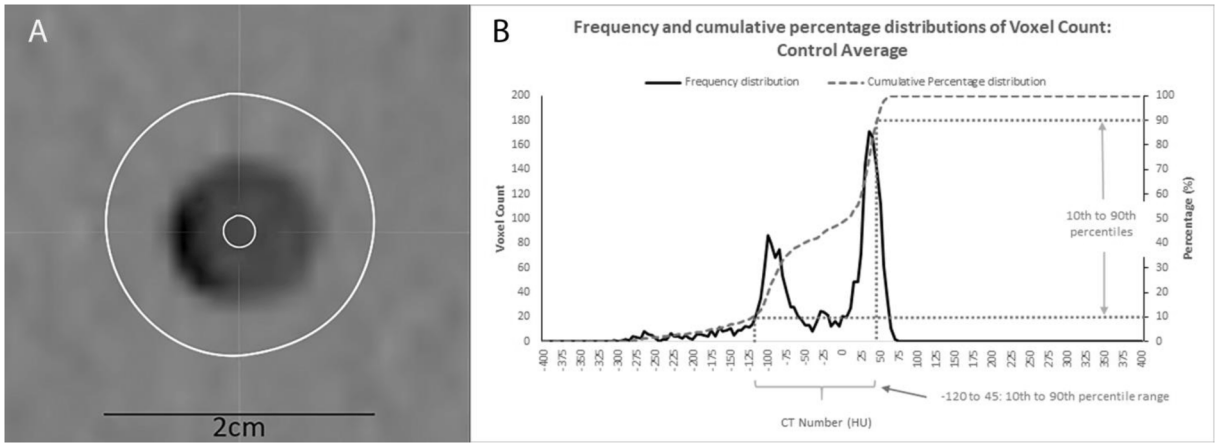

Fig. 2. Phantom Model Artefact Analysis: Example of Histogram and Cumulative percentage distribution of voxel count and calculated Percentile Range by CT number Hounsfield Unit (HU) for Wax Control illustrating A) Cross-section through the wax block control inserted in the phantom. The outer contour is the 2 cm sphere, while the inner contour denotes the fiducial volume equivalent to the gold or small glue fiducial. B) The corresponding histogram represents the CT number (HU) versus voxel count for the 2 cm sphere minus the fiducial volume used to calculate the artefact analysis's percentile ranges.

3.2. Phantom fiducial characterization

The fiducials were analyzed separately from the surrounding phantom and artifact (Table 1). Notably, the fiducials are small relative to the sphere; they occupied only 6 to 38 voxels compared to 1912 sphere voxels of the sphere. The wax control, gold, EO alone, and small glue fiducials had the same volume and similar voxel count. The wax control had median CT number values 48 HU lower than the surrounding phantom but was still within the normal tissue-equivalent range. Therefore, this should not affect the results based on the percentile ranges and percentage of voxels in the normal tissue range. Some wax blocks had incomplete thin rims of air, low CT number voxels adjacent to the phantom interface (Fig. 3). However, these represented only a small proportion of the sphere and did affect the results. EO alone was designed to have the same volume as the small glue fiducials and had comparable CT number characteristics to the glue fiducials (Table 1).

The gold fiducial was the same size as the small glue fiducials but had a greater contrast with 12 to 16 times greater CT number values than the small EO fiducials. The glue did not impact the CT number characteristics of the EO. The differences in median CT number between the glue fiducial and EO alone was 28–142 HU. Both the smaller EC and EM fiducials had similar CT number characteristics, with the differences in their median CT number values being 114 HU. The larger EC and EM fiducials were similar, but both exhibited greater median CT number values than the smaller counterparts but were not as high as gold.

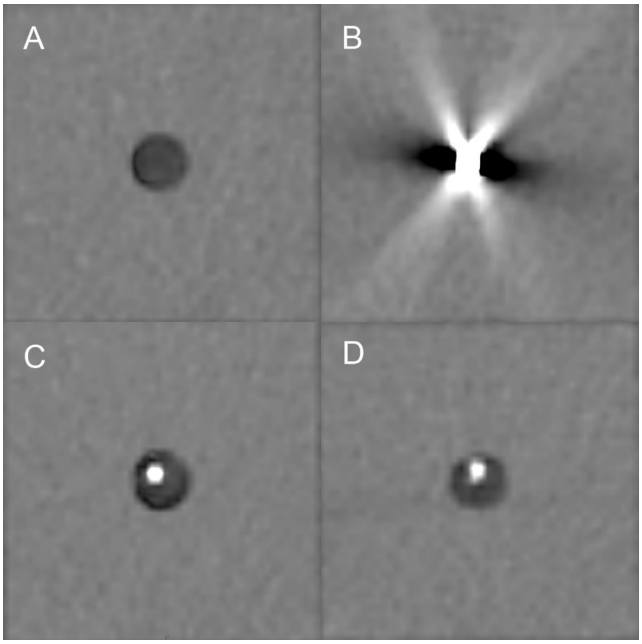

Fig. 3. Phantom Model: CT scan of phantom showing A) Wax control – normal tissue density but less dense than the phantom, B) Gold fiducial and artifact, C) Small EC fiducial, and D) Small EM. The EO glue fiducials C) and D) have a minimal artifact. Abbreviations: EC: ethiodized oil and monomeric n-butyl-2-cyanoacrylate, EM: ethiodized oil and n-butyl cyanoacrylate and meth-acryloxysulpholen monomers, EO: ethiodized oil.

3.3. Phantom fiducial artefact characterization

Sphere voxels were mostly normal tissue density. The bright and dark artifacts result in the HU voxel variation outside the normal tissue range at the extreme high and low HU values, respectively, at the histogram ends, i.e., bright radiating or dark shadowing artifact. The greater spread of the histogram, the less normal tissue is represented as it is obscured by the high or low HU artifact from the fiducials.

The gold fiducial sphere CT number values for the 1st to 99 percentile ranges were 593, 604, and 600 HU greater than small EC, EM, and EO alone fiducials, respectively, and 563 HU greater than the control (Table 2). This suggested a larger number of voxels being present at the extreme ends of the CT number histogram and is representative of an increased artifact for the gold fiducials (Fig. 3B, Fig. 4).

Both glue fiducials showed similar CT number values across the percentile ranges, with differences between 1 and 11HU for the small fiducials and 0 to 42 HU for the larger glue fiducials. There were also only small differences from the wax control, indicating that the artifact was minimal (Table 2, Fig. 3 C & D, Fig. 4). The tissue glue did not affect the fiducials' CT number artifact characteristics, with differences between the small EC and EO ranging from 1 to 7 HU and 2 to 10 HU for the small EM fiducial (Table 2). The remaining percentile ranges and percentage of voxels in the designated normal tissue ranges only showed minor differences, indicating that the artifacts made up only a small proportion of the 2 cm spheres.

Compared to the smaller glue fiducial, the larger glue fiducial's CT number histogram spread was greater for the 1st to 99 percentile range but less than gold. There were only minor variations in values between the EC and EM fiducials for all other values.

Table 2
Phantom Model: Artefact Analysis – Mean and Standard Deviations (SD) of Percentile ranges of the CT number Hounsfield Unit (HU) versus voxels count histograms and proportion of voxels within normal tissue CT number HU range for 2 cm spheres surrounding the fiducial. It illustrates that the glue fiducials produce fewer artifacts than gold with smaller percentile ranges and a greater percentage of voxels in normal tissue range +/−100 and +/−150 HU. Abbreviations: EO: ethiodized oil, EC: ethiodized oil and monomeric n-butyl-2-cyanoacrylate, EM: ethiodized oil and n-butyl cyanoacrylate and methacryloxysulpholen monomers.

Sphere/ Factor	Number Of Fiducials Spheres	1st to 99th percentile, mean (SD)	5th to 95th percentile, mean (SD)	10th to 90th percentile, mean (SD)	25th to 75th percentile, mean (SD)	Percentage within +/−100 HU, mean (SD)	Percentage within +/−150 HU, mean (SD)
Control (Wax)	2	310 (21)	200 (35)	163 (4)	128 (4)	78 (2)	95 (3)
EO alone	2	273 (11)	215 (14)	175 (7)	133 (4)	75 (3)	92 (1)
Gold	2	873 (110)	270 (57)	173 (11)	128 (4)	74 (1)	91 (2)
Small EC	4	280 (30)	211 (10)	174 (5)	131 (5)	76 (2)	93 (1)
Small EM	4	269 (39)	205 (32)	178 (21)	135 (9)	73 (6)	94 (5)
Large EC	2	360 (35)	203 (4)	165 (0)	123 (4)	80 (1)	94 (0)
Large EM	2	318 (32)	180 (7)	158 (4)	123 (4)	79 (1)	97 (1)

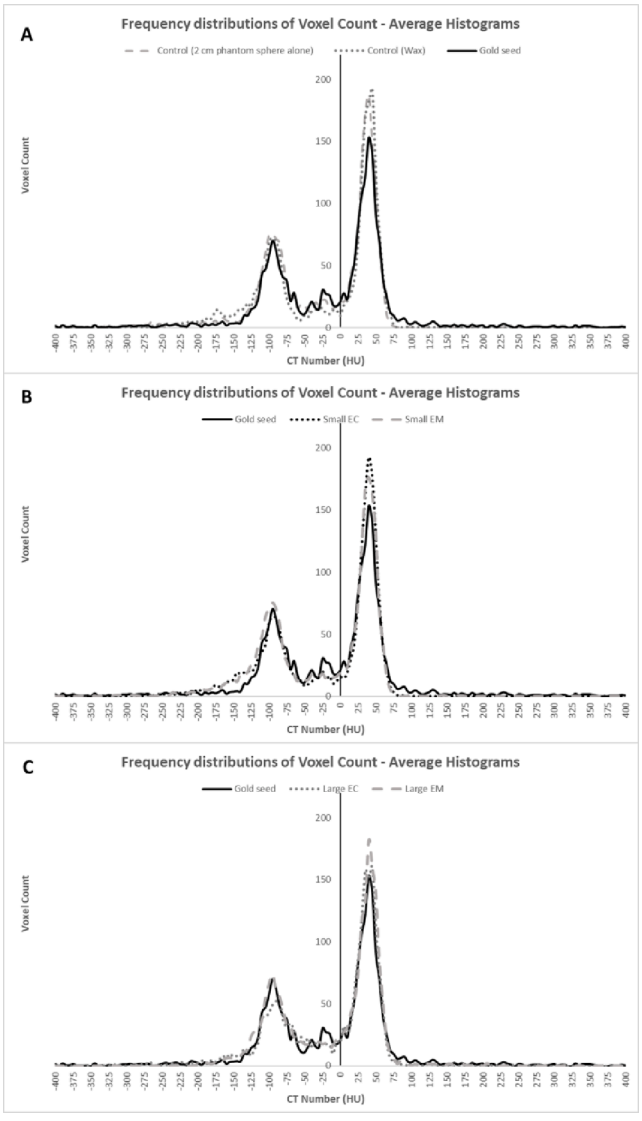

Fig. 4. Phantom Model Artefact Analysis: Average Histograms (Frequency Distribution) of voxel count by CT number Hounsfield Unit (HU) for a 2 cm sphere minus the fiducial volume illustrating A) Control (2 cm phantom sphere alone), Control (wax) and Gold fiducial; B) Gold fiducial, Small EC and Small EM; and C) Gold fiducial, Large EC and Large EM. Abbreviations: EC: ethiodized oil and monomeric n-butyl-2-cyanoacrylate, EM: ethiodized oil and n-butyl cyanoacrylate and methacryloxysulpholen monomers.

4. Discussion

This study has confirmed that glue fiducials can be delivered cystoscopically into a fluid-filled bladder and produce a discrete visible marker with minimal artifact compared to standard gold fiducials and thus suitable for image guidance. However, the glue fiducials were larger than the gold markers but had comparable imaging and artifact characteristics to EO alone.

Fiducials, in an imaged guided approach, are critical for targeting in partial bladder radiotherapy to treat the bladder tumor alone or as part of a dose-escalation boost [17,18]. The bladder can greatly distend, particularly in the cranial-caudal direction. Margins of two to three cm are required to account for this distension, potentially resulting in increased bowel toxicity [19,20]. However, studies that use EO or gold fiducials for partial bladder radiotherapy utilize smaller anisotropic PTV margins of 5 mm–15 mm [4,5,17,21].

Investigations have shown that EO fiducials effectively define the tumor within the bladder for image guidance [4,5,17]. A recent study using cone-beam verification has shown that EO resulted in a higher interobserver agreement than bladder wall surface matching and decreased PTV margins [22]. However, there was a substantial shape variation of the EO markers due to bladder filling [22].

While the EO only markers can fade, they exhibit a high retention rate and remain visible throughout radiotherapy. However, the ability to use them for radiotherapy verification is variable. In terms of verification with EO, success rates have been reported to be between 76% and 100% [23]. Chai et al. reported that 92% of the markers remained in situ after the radiation course in 15 patients. However, a further 16 patients could not be included in the series as the fiducials could not be registered for image-guided therapy due to splitting or joining [24]. Thus, there is a learning curve to achieve EO markers suitable for radiotherapy verification [5]. Despite success in achieving discrete visible EO fiducials, our experience when using EO alone has been inconsistent. EO dispersion through and beyond the bladder wall into peri-vesical tissue sometimes limited its specificity as a fiducial marker and prompted our investigation of tissue glues.

Side effects of EO, including an allergic reaction, are uncommon and mostly transient [17]. The studies of EO bladder markers have not reported any significant toxicity [25]. The EO and CA combination has been utilized in multiple sites, with infrequent, serious side effects [9,26]. More specifically, CA and CM glues have been used in urological procedures, including animal urethral tissue models, urinary fistulas [27], and the treatment of persistent anastomotic urine leaks after radical prostatectomy [28].

Gold has also been used as fiducials for partial bladder and post-prostatectomy radiotherapy [1,21,29,30]. Gold is easily visible on X-ray imaging due to its high Z value. However, this subsequently causes bright radiating and dark shadowing metal artifact [25], resulting in the inaccurate fiducial definition that interferes with precise verification.

The artifact can also obscure the anatomy causing difficulties in target delineation. Another significant but uncommon risk with the combination of surgery, radiotherapy, and foreign body include fistulae [31,32]. A further issue is the drop-out rate, which is estimated to be 50%, particularly from the tumor area [5,29,33]. There have also been technical difficulties inserting gold fiducials into the bladder dome [29].

The caveats of EO alone and gold fiducials markers have led us to investigate the EO glue combinations. EO and tissue glue (CA or CM) are generally available in most surgical hospitals. EO and CA mixture is a less expensive combination [34]. The glue fiducials have good visibility in various imaging modalities, minimal distortion in CT imaging, minimal dose perturbation, and are biocompatible with soft tissue. The widespread use of EO and tissue glues indicates that they can be safely used in many anatomical sites.

The study did not investigate artifact suppression CT for the gold fiducials [35,36] or alternative markers, including newer commercially available liquid gel fiducials that have recently been trialed in the bladder, such as BioXmark (sucrose acetate isobutyrate (SAIB), iodinated SAIB, and ethanol solution) [37] or TraceIT (iodinated polyethylene glycol microparticles, hydrogel) [34]. We have found that glue fiducials and TraceIT [34] have their pros and cons. At our center, the CA and EO are readily available and less expensive. However, the relative utility of different liquid fiducials can only be resolved in a comparative study that is under consideration.

Interestingly, EO produces high signal intensity on T1-weighted MRI images and low signal intensity on T2-weighted images [38]. A future interest will be to develop fiducials for MRI, possibly using EO or another MRI contrast agent with tissue glue. A comparison with TraceIT or BioXmark would also be appropriate, as both are marketed as being visible on MRI.

The study was an ex vivo and in vitro investigation of glue fiducials where they were imaged immediately after insertion. Issues such as fading, retention, distortion, migration, and dispersion resulting from normal physiological processes during radiotherapy are more appropriately assessed in a clinical study. However, these issues were not evident in our previous gastro-oesophageal patient study [9] or earlier investigations of EO alone (except dispersion). An in vivo study is planned to address the clinical and imaging aspects, including the fiducials' durability, CBCT, MRI, and workflow aspects in a patient population undergoing bladder radiotherapy.

In conclusion, the study has confirmed the potential use of EO glue fiducials for radiotherapy bladder targeting. They have advantages over gold markers in terms of decreased artifact production and maybe more easily deliverable with less dispersion than EO alone. The components are readily available, and the EO Histoacryl mixture is relatively inexpensive. Patient studies are warranted to assess the utility and durability of these fiducials during a radiotherapy course.

Declaration of Competing Interest

The authors declare the following financial interests/personal relationships which may be considered as potential competing interests: Providers: KARL STORZ Endoscopy Australia Pty Ltd supplied the cystoscopes, William A. Cook Australia PTY LTD supplied the Williams Cystoscopic Injection needles, Guerbet USA supplied the Lipiodol Ethiodized Oil, B.Braun Australia Pty.Ltd supplied the Histoacryl, MatrixSurgical supplied the Glubran2 (GEM), Sinclair's Abattoir, Benalla Victoria, supplied the pig bladders and Brenta's Butcher, Fairfield Victoria supplied the pigs pelvis.

Acknowledgments

Radiotherapy Nursing for their support for the procedure and the providers: KARL STORZ Endoscopy Australia Pty Ltd supplied the cystoscopes, William A. Cook Australia PTY LTD supplied the Williams Cystoscopic Injection needles, Guerbet USA supplied the Lipiodol (EO Ethiodized Oil), B.Braun Australia Pty. Ltd supplied the Histoacryl, MatrixSurgical supplied the Glubran2 (GEM), Sinclair's Abattoir, Benalla Victoria, supplied the pig bladders and Brenta's Butcher, Fairfield Victoria supplied the pigs pelvis.

References

[1] Shakir SI, Udrescu C, Enachescu C, Rouviere O, Arion S, Caraivan I, et al. Transrectal implantation and stability of gold markers in prostate bed for salvage radiotherapy of macroscopic recurrences. Phys Med 2016;32:1422–7. https://doi.org/10.1016/j.ejmp.2016.10.009.
[2] Barrett JF, Keat N. Artifacts in CT: recognition and avoidance. Radiographics 2004; 24:1679–91. https://doi.org/10.1148/rg.246045065.
[3] Gjesteby L, De Man B, Jin Y, Paganetti H, Verburg J, Giantsoudi D, et al. Metal artifact reduction in CT: Where are we after four decades? IEEE Access 2016;4: 5826–49. https://doi.org/10.1109/access.2016.2608621.
[4] Pos F, Bex A, Dees-Ribbers HM, Betgen A, van Herk M, Remeijer P. Lipiodol injection for target volume delineation and image guidance during radiotherapy for bladder cancer. Radiother Oncol 2009;93:364–7. https://doi.org/10.1016/j.radonc.2009.09.003.
[5] Søndergaard J, Olsen KØ, Muren LP, Elstrøm UV, Grau C, Høyer M. A study of image-guided radiotherapy of bladder cancer based on lipiodol injection in the bladder wall. Acta Oncol 2010;49:1109–15. https://doi.org/10.3109/02841861003789491.
[6] Committee AT, Bhat YM, Banerjee S, Barth BA, Chauhan SS, Gottlieb KT, et al. Tissue adhesives: cyanoacrylate glue and fibrin sealant. Gastrointest Endosc 2013; 78:209–15. https://doi.org/10.1016/j.gie.2013.04.166.
[7] Weil D, Cervoni JP, Fares N, Rudler M, Bureau C, Plessier A, et al. Management of gastric varices: a French national survey. Eur J Gastroenterol Hepatol 2016;28: 576–81. https://doi.org/10.1097/MEG.0000000000000560.
[8] Loh DC, Wilson RB. Endoscopic management of refractory gastrointestinal non-variceal bleeding using Histoacryl (N-butyl-2-cyanoacrylate) glue. Gastroenterol Rep (Oxf) 2016;4:232–6. https://doi.org/10.1093/gastro/gov019.
[9] Chandran S, Vaughan R, Jacob A, Hamilton C, Joon DL, Lim K, et al. A novel endoscopic marker for radiological localization and image-guided radiotherapy in esophageal and gastric cancers (with video). Gastrointest Endosc 2016;83:309–17. https://doi.org/10.1016/j.gie.2015.06.042.
[10] Cheng LF, Wang ZQ, Li CZ, Lin W, Yeo AE, Jin B. Low incidence of complications from endoscopic gastric variceal obturation with butyl cyanoacrylate. Clin Gastroenterol Hepatol 2010;8:760–6. https://doi.org/10.1016/j.cgh.2010.05.019.
[11] Duncan C, Joon DL, Lawrentschuk N, Jenkins T, Schneider M, Khoo V, et al. Fiducial markers: can the urologist do better? World J Urol 2019;37:1281–7. https://doi.org/10.1007/s00345-018-2515-0.
[12] Lim HK, Ha HI, Park SY, Lee K. Comparison of the diagnostic performance of CT Hounsfield unit histogram analysis and dual-energy X-ray absorptiometry in predicting osteoporosis of the femur. Eur Radiol 2019;29:1831–40. https://doi.org/10.1007/s00330-018-5728-0.
[13] Paul J, Yang C, Wu H, Tai A, Dalah E, Zheng C, et al. Early assessment of treatment responses during radiation therapy for lung cancer using quantitative analysis of daily computed tomography. Int J Radiat Oncol Biol Phys 2017;98:463–72. https://doi.org/10.1016/j.ijrobp.2017.02.032.
[14] Zhang LX, Xiang JJ, Wei PY, Ding JW, Luo DC, Peng ZY, et al. Diagnostic value of computed tomography (CT) histogram analysis in thyroid benign solitary coarse calcification nodules. J Zhejiang Univ Sci B 2018;19:211–7. https://doi.org/10.1631/jzus.B1700119.
[15] Gonzalez RC, Woods RE. Some Basic Intensity Transformation Functions. In Digital Image Processing, 4th Edition. 4 ed: Pearson; 2018. p. 139-42.
[16] Zhou Y, Shi C, Lai B, Jimenez G. Contrast enhancement of medical images using a new version of the World Cup Optimization algorithm. Quant Imaging Med Surg 2019;9:1528–47. https://doi.org/10.21037/qims.2019.08.19.
[17] Freilich JM, Spiess PE, Biagioli MC, Fernandez DC, Shi EJ, Hunt DC, et al. Lipiodol as a fiducial marker for image-guided radiation therapy for bladder cancer. Int Braz J Urol 2014;40:190–7. https://doi.org/10.1590/S1677-5538.IBJU.2014.02.08.
[18] Muren LP, Redpath AT, McLaren D, Rorvik J, Halvorsen OJ, Hostmark J, et al. A concomitant tumour boost in bladder irradiation: patient suitability and the potential of intensity-modulated radiotherapy. Radiother Oncol 2006;80:98–105. https://doi.org/10.1016/j.radonc.2006.06.015.
[19] Pos F, Remeijer P. Adaptive management of bladder cancer radiotherapy. Semin Radiat Oncol 2010;20:116–20. https://doi.org/10.1016/j.semradonc.2009.11.005.
[20] Muren LP, Smaaland R, Dahl O. Organ motion, set-up variation and treatment margins in radical radiotherapy of urinary bladder cancer. Radiother Oncol 2003; 69:291–304. https://doi.org/10.1016/S0167-8140(03)00246-9.
[21] Fortin I, Carrier JF, Beauchemin MC, Beliveau-Nadeau D, Delouya G, Taussky D. Using fiducial markers in the prostate bed in postprostatectomy external beam radiation therapy improves accuracy over surgical clips. Strahlenther Onkol 2014; 190:467–71. https://doi.org/10.1007/s00066-014-0631-3.
[22] Kong V, Kwan M, Chen S, Chung P, Craig T, Rosewall T. Quantification of interobserver variability in image registration using cone beam CT for partial bladder radiotherapy—a comparison between lipiodol and bladder wall surface. Br J Radiol 2019;92:20180413. https://doi.org/10.1259/bjr.20180413.
[23] Kliton J, Polgar C, Tenke P, Kovacs G, Major T, Stelczer G, et al. Image-guided radiotherapy for muscle invasive bladder cancer with intravesical lipiodol

injection. A new option for bladder sparing treatment. Orv Hetil 2017;158:2041–7. https://doi.org/10.1556/650.2017.30904.
[24] Chai X, van Herk M, van de Kamer JB, Remeijer P, Bex A, Betgen A, et al. Behavior of lipiodol markers during image guided radiotherapy of bladder cancer. Int J Radiat Oncol Biol Phys 2010;77:309–14. https://doi.org/10.1016/j.ijrobp.2009.08.019.
[25] Nolan CP, Forde EJ. A review of the use of fiducial markers for image-guided bladder radiotherapy. Acta Oncol 2016;55:533–8. https://doi.org/10.3109/0284186X.2015.1110250.
[26] Machiels M, Voncken FEM, Jin P, van Dieren JM, Bartels-Rutten A, Alderliesten T, et al. A novel liquid fiducial marker in esophageal cancer image guided radiation therapy: technical feasibility and visibility on imaging. Pract Radiat Oncol 2019;9:e506–15. https://doi.org/10.1016/j.prro.2019.06.018.
[27] Ayyildiz SN, Ayyildiz A. Cyanoacrylic tissue glues: biochemical properties and their usage in urology. Turk J Urol 2017;43:14–24. https://doi.org/10.5152/tud.2017.09465.
[28] Lim JH, You D, Jeong IG, Park HK, Ahn H, Kim CS. Cystoscopic injection of N-butyl-2-cyanoacrylate followed by fibrin glue for the treatment of persistent or massive vesicourethral anastomotic urine leak after radical prostatectomy. Int J Urol 2013;20:980–5. https://doi.org/10.1111/iju.12094.
[29] Mangar S, Thompson A, Miles E, Huddart R, Horwich A, Khoo V. A feasibility study of using gold seeds as fiducial markers for bladder localization during radical radiotherapy. Br J Radiol 2007;80:279–83. https://doi.org/10.1259/bjr/54321311.
[30] Langenhuijsen JF, Donker R, McColl GM, Kiemeney LA, Witjes JA, van Lin EN. Postprostatectomy ultrasound-guided transrectal implantation of gold markers for external beam radiotherapy. Technique and complications rate. Strahlenther Onkol 2013;189:476–81. https://doi.org/10.1007/s00066-013-0323-4.
[31] Borchers H, Pinkawa M, Donner A, Wolter TP, Pallua N, Eble MJ, et al. Rectourethral fistula following LDR brachytherapy. Urol Int 2009;82:365–6. https://doi.org/10.1159/000209374.
[32] Chao M, Ho H, Chan Y, Tan A, Pham T, Bolton D, et al. Prospective analysis of hydrogel spacer for patients with prostate cancer undergoing radiotherapy. BJU Int 2018;122:427–33. https://doi.org/10.1111/bju.14192.
[33] Hulshof MC, van Andel G, Bel A, Gangel P, van de Kamer JB. Intravesical markers for delineation of target volume during external focal irradiation of bladder carcinomas. Radiother Oncol 2007;84:49–51. https://doi.org/10.1016/j.radonc.2007.05.017.
[34] Chao M, Ho H, Joon DL, Chan Y, Spencer S, Ng M, et al. The use of tissue fiducial markers in improving the accuracy of post-prostatectomy radiotherapy. Radiat Oncol J 2019;37:43–50. https://doi.org/10.3857/roj.2018.00556.
[35] Wei J, Sandison GA, Hsi WC, Ringor M, Lu X. Dosimetric impact of a CT metal artefact suppression algorithm for proton, electron and photon therapies. Phys Med Biol 2006;51:5183–97. https://doi.org/10.1088/0031-9155/51/20/007.
[36] Chan MF, Cohen GN, Deasy JO. Qualitative evaluation of fiducial markers for radiotherapy imaging. Technol Cancer Res Treat 2015;14:298–304. https://doi.org/10.1177/1533034614547447.
[37] de Ridder M, Gerbrandy LC, de Reijke TM, Hinnen KA, Hulshof M. BioXmark(R) liquid fiducial markers for image-guided radiotherapy in muscle invasive bladder cancer: a safety and performance trial. Br J Radiol 2020;93:20200241. https://doi.org/10.1259/bjr.20200241.
[38] Santis MD, Alborino S, Tartoni PL, Torricelli P, Casolo A, Romagnoli R. Effects of lipiodol retention on MRI signal intensity from hepatocellular carcinoma and surrounding liver treated by chemoembolization. Eur Radiol 1997;7:10–6. https://doi.org/10.1007/s003300050099.